**Human Reproduction, Vol.00, No.0, pp. 1–15, 2021**
doi:10.1093/humrep/deab080

human reproduction

**ORIGINAL ARTICLE** ***Reproductive genetics***

# Non-invasive preimplantation genetic testing for putative mosaic blastocysts: a pilot study

**Xinyuan Li [1,2,3,†], Yan Hao [1,2,3,†], Dawei Chen [1,4,5], Dongmei Ji [1,4,5], Wanbo Zhu [6], Xiaoqian Zhu [1,4,5], Zhaolian Wei [1,4,5], Yunxia Cao [1,4,5], Zhiguo Zhang [1,2,3,*], and Ping Zhou [1,2,3,*]**

[1]Department of Obstetrics and Gynecology, Reproductive Medicine Center, the First Affiliated Hospital of Anhui Medical University, Anhui, China [2]NHC Key Laboratory of Study on Abnormal Gametes and Reproductive Tract, Anhui Medical University, Hefei, Anhui, China [3]Key Laboratory of Population Health Across Life Cycle, Anhui Medical University, Ministry of Education of the People's Republic of China, Hefei, Anhui, China [4]Anhui Province Key Laboratory of Reproductive Health and Genetics, Hefei, Anhui, China [5]Biopreservation and Artificial Organs, Anhui Provincial Engineering Research Center, Anhui Medical University, Hefei, Anhui, China [6]Affiliated Anhui Provincial Hospital of Anhui Medical University, Anhui, China

*Correspondence address. Department of Obstetrics and Gynecology, Reproductive Medicine Center, the First Affiliated Hospital of Anhui Medical University, No 218 Jixi Road, Hefei, Anhui 230022, China. Tel: +86-13965042605; E-mail: zhouping6292@126.com https://orcid.org/0000-0001-8125-3525 (P.Z.); Tel: +86-18155106683; E-mail: zzg_100@163.com https://orcid.org/0000-0003-1483-3321 (Z.Z.)

*Submitted on July 14, 2020; resubmitted on March 6, 2021; editorial decision on March 10, 2021*

**STUDY QUESTION:** What is the potential of applying non-invasive preimplantation genetic testing (niPGT) for chromosome abnormalities in blastocysts reported with a mosaic trophectoderm (TE) biopsy?

**SUMMARY ANSWER:** niPGT of cell-free DNA in blastocyst culture medium exhibited a good diagnostic performance in putative mosaic blastocysts.

**WHAT IS KNOWN ALREADY:** Advances in niPGT have demonstrated the potential reliability of cell-free DNA as a resource for genetic assessment, but information on mosaic embryos is scarce because the mosaicism may interfere with niPGT. In addition, the high incidence of mosaicism reported in the context of PGT and the viability of mosaic blastocysts raise questions about whether mosaicism really exists.

**STUDY DESIGN, SIZE, DURATION:** The study was performed between May 2020 and July 2020. First, clinical data collected by a single-center over a 6-year period on PGT for chromosome aneuploidies (PGT-A) or chromosomal structural rearrangements (PGT-SR) were analyzed. After confirming the reliability of niPGT, 41 blastocysts classified as mosaics by trophectoderm (TE) biopsy were re-cultured. The chromosomal copy number of the blastocyst embryo (BE, the gold standard), TE re-biopsy, and corresponding cell-free DNA in the culture medium was assessed.

**PARTICIPANTS/MATERIALS, SETTING, METHODS:** Data on patients enrolled for PGT at a single center from 2014 to 2019 were collected and the cycles with available putative mosaic blastocysts were evaluated. To verify the diagnostic validity of niPGT, eight aneuploid blastocysts were thawed and re-cultured for 14–18 h. The concordance of the niPGT diagnosis results and the whole blastocyst testing results was analyzed. Forty-one blastocysts reported as mosaics from 22 patients were included and re-cultured for 14–18 h. The genetic material of the BE, TE re-biopsy, and corresponding cell-free DNA in the culture medium was amplified using multiple annealing and looping-based amplification cycles. The karyotype data from niPGT and TE re-biopsy were compared with that from the whole blastocyst, and the efficiency of niPGT was assessed.

**MAIN RESULTS AND THE ROLE OF CHANCE:** Data on 3738 blastocysts from 785 PGT-A or PGT-SR cycles of 677 patients were collected. According to the TE biopsy report, of the 3662 (98%) successfully amplified samples, 24 (0.6%) yielded no results, 849 (23.2%) were euploid, 2245 (61.3%) were aneuploid, and 544 (14.9%) were mosaic. Sixty patients without euploid blastocysts opted for a single mosaic blastocyst transfer, and 30 (50%) of them obtained a clinical pregnancy. With the BE chromosome copy number as the gold standard, niPGT and TE re-biopsy showed reliable detection ability and diagnostic efficiency in eight putative aneuploid blastocysts. Of the 41 putative mosaic blastocysts re-cultured and re-tested, 35 (85.4%) showed euploid BE results. All but two of the blastocysts previously diagnosed with segmental chromosomal mosaic were actually euploid. In addition, all blastocysts previously classified as low degree

[†]The authors consider that the first two authors should be regarded as joint first authors.

(20–50%) mosaics were identified as euploid by BE PGT, whereas four of the six putative high degree (50–80%) mosaic blastocysts showed chromosomal abnormalities. The raw concordance rates of spent culture medium (SCM) and TE re-biopsies compared with BE were 74.4% and 82%, respectively, in terms of overall ploidy and 96.2% and 97.6%, respectively, per single chromosome when considering all degree mosaic results as true positives. However, when we set a mosaicism identification threshold of 50%, the concordance rates of SCM and TE re-biopsies compared with BE were 87.2% and 85% at the overall ploidy level and 98.8% and 98.3% at the chromosomal level, respectively. At the full ploidy level, the sensitivity and false negative rates for niPGT were 100% and 0, respectively. After adjustment of the threshold for mosaicism, the specificity of niPGT increased from 69.7% to 84.8% in terms of overall ploidy and from 96.1% to 98.9% at the chromosomal level.

**LIMITATIONS, REASONS FOR CAUTION:** The primary limitation of this study is the small sample size, which decreases the strength of our conclusions. If possible, identifying the clinical outcome of niPGT on reassessed mosaic blastocysts would be further progress in this field.

**WIDER IMPLICATIONS OF THE FINDINGS:** This study is the first to explore the practicability of niPGT in diagnostic reassessment of putative mosaicism. The present study provides a novel opportunity for patients with only mosaic blastocysts and no euploid blastocysts, regardless of the technical or biological basis of mosaicism. Employing niPGT after 14–18 h of re-culturing might be a superior option for the best use of blastocysts because of its minimally invasive nature.

**STUDY FUNDING/COMPETING INTEREST(S):** This work was supported by grants from National Key Technology Research and Development Program of China (No. 2017YFC1002004), the Central Guiding the Science and Technology Development of the Local (2018080802D0081) and College Natural Science Project of Anhui Province (KJ2019A0287). There are no competing interests to declare.

**TRIAL REGISTRATION NUMBER:** N/A

**Key words:** non-invasive preimplantation genetic testing/ mosaicism/ preimplantation genetic testing for aneuploidies/ segmental aneuploidy/ culture medium

# Introduction

Preimplantation genetic testing (PGT) for patients with or without a chromosomal abnormality is considered a robust and standard diagnostic test that takes full advantage of competent embryos. PGT methods based on biopsy of polar bodies obtained from oocytes, blastomeres from cleavage stage embryos, and trophectoderm (TE) cells from blastocysts have been demonstrated to yield acceptable pregnancy outcomes (De Rycke *et al.*, 2017). However, the invasive nature of these methods poses a potential threat to subsequent development of biopsied embryos. Moreover, highly skilled embryologists and special equipment are required for the manipulations during biopsy, thereby increasing costs and discouraging many clinics from conducting PGT program. Next-generation sequencing (NGS) combined with TE biopsy is currently the most widely used method for PGT. However, its use is limited by the uncertainty surrounding the question of whether sampling of cells from TE is a good representation of the whole blastocyst. Although several publications have reported a consistency between TE and the inner cell mass (ICM) (Vera-Rodriguez *et al.*, 2016; Fragouli *et al.*, 2017; Chuang *et al.*, 2018), others have suggested the opposite with a hypothesis of preferential allocation of euploid cells to the ICM (Liu *et al.*, 2012). Likewise, the presence of mosaicism has further affected the reliability and accuracy of using a single biopsy of only 5–10 TE cells (Gleicher *et al.*, 2017).

In the last few years, an innovative non-invasive method that depends on sampling genetic material from spent culture medium (SCM) has emerged. Non-invasive PGT (niPGT) paves the way for the selection of viable embryos while posing minimal risk to the development of the embryos. With the improvement and optimization of whole genome amplification protocols, the amplification rate of cell-free DNA has increased from 35% to 82% (when using blastocoele fluid, BF) to 100% (with the combined use of BF and SCM) (Palini *et al.*, 2013; Magli *et al.*, 2016; Xu *et al.*, 2016; Capalbo *et al.*, 2018; Yeung *et al.*, 2019). Meanwhile, the overall ploidy and full chromosome concordance are generally acceptable for PGT for aneuploidies (PGT-A), indicating the potential reliability of cell-free DNA as a resource for genetic assessment at the level of chromosome copy number (Leaver and Wells, 2020).

A large number of related achievements have promoted the clinical application of niPGT (Xu *et al.*, 2016; Leaver and Wells, 2020; Rubio *et al.*, 2020). However, the significant heterogeneity of results reported in the literature has limited this protocol from being brought into the clinical sphere. On the other hand, studies have focused on embryos with aneuploidy or an unknown karyotype, and information associated with mosaic embryos is scarce because the presence of mosaicism may interfere with niPGT (Popovic *et al.*, 2020). Studies focused on clinical outcomes of mosaic embryo transfer have revealed the developmental potential of these embryos and suggested that such embryos should be considered as suboptimal alternatives, rather than be discarded (Greco *et al.*, 2015; Munne *et al.*, 2017). The mechanism(s) underlying mosaicism remains elusive, and the genetic material obtained from SCM of mosaic embryos is undefined and could result in false positive results. One study hypothesized that cell-free DNA is more reliable than TE biopsy for diagnosing mosaic embryos because the genetic material is released into culture media from both ICM and TE cell lineages (Huang *et al.*, 2019a). Based on this theory, in the present study, we thawed and re-cultured frozen blastocysts that were considered as mosaics after PGT-A or PGT for chromosomal structural rearrangements (PGT-SR) in order to explore the clinical application value of niPGT in putative mosaic blastocysts and the potential mechanism of mosaicism. TE re-biopsy, blastocyst embryos (BE), and corresponding SCM were collected to assess chromosomal abnormalities. We considered the ploidy and chromosome copy number of BE as the gold standard for comparing with corresponding TE re-biopsy, SCM, and previous TE biopsy results.

# Materials and methods

## Ethics statement

This study was approved by the Ethics Committee of Anhui Medical University (Hefei, China; Approval No. 20191226) and all participants provided informed consent. The clinical viability and potential risk of transferring mosaic blastocysts had been stated clearly in the informed consent. All patients who donated blastocysts with a mosaic diagnosis for this study have had a healthy baby after transfer of a euploid blastocyst.

## Clinical sample collection

Data from patients enrolled for PGT-A or PGT-SR at the Reproductive Medical Center of the First Affiliated Hospital of Anhui Medical University from 2014 to 2019 were included, and the cycles with available mosaic blastocysts were evaluated. Laboratory and clinical outcomes of these cycles were analyzed. We performed PGT using comprehensive 24-chromosomal copy number detection methods. Array comparative genomic hybridization (aCGH) was used between 2014 and 2017 but was subsequently replaced by the more sensitive next-generation sequencing (NGS) platform.

## Routine protocol for PGT

All retrieved mature oocytes of patients included in PGT cycles were fertilized by ICSI. Oocytes were placed in a 30 μl microdroplet of cleavage culture medium (COOK, Queensland, Australia) with 10% serum substitute supplement (SSS) (IrvineScientific, Santa Ana, CA, USA) and covered with mineral oil. On Day 3 post-fertilization, normally fertilized and cleaved embryos were individually transferred into a 30 μl microdroplet of blastocyst culture medium (COOK, Queensland, Australia) with 10% SSS. Each embryo was assessed on Day 5 or 6 until the formation of a high-quality blastocyst (Gardner *et al.*, 1998). Biopsy was performed in a specific dish containing 7.5 μl blastocyst medium. Laser-assisted breaking of the zone pellucida using an infrared laser (Hamilton Thorne LYKOS, Beverly, MA, USA) and removal of 5–10 TE cells using an aspiration pipette (30 μm inner diameter) were performed on the TE side, distant from the ICM. The remaining blastocysts were vitrified individually. Each biopsied sample was transferred into a PCR tube and stored at −80◦C before being sent for PGT.

Samples obtained from the TE biopsy underwent whole genome amplification (WGA) according to the instructions of the Sureplex DNA Amplification System (BlueGnome, Cambridge, UK). For aCGH, the WGA products were labeled with CY3–CY5 and hybridized with a BlueGnome 24syre V3 chip according to the specification of the BlueGmone 24sure V3 package kit (BlueGnome, Cambridge, UK). The chip was scanned by Innoscan710 scanner after washing, and the optical signals were analyzed by BlueFuse MulTI software (BlueGnome, Cambridge, UK). For NGS, the WGA products were purified and then used for library preparation with an Ion Xpress™ Plus Fragment Library Kit (Life Technologies, Grand Island, NY, USA). The sequencing template preparation was performed using an Ion One Touch 2 system and an Ion One Touch ES following instructions in the latest version of the Ion OneTouch 200 Template kit (Life Technologies, Grand Island, NY, USA). High-throughput sequencing and analysis were performed with an Ion Proton 200 Sequencing Kit (Life Technologies, Grand Island, NY, USA) (Elshewy *et al.*, 2020).

## Blastocyst thawing and re-culture

Forty-one blastocysts classified as mosaic by previous TE biopsy from 22 patients were included. Of the 22 patients, 9 had a chromosomal reciprocal translocation in their karyotype, 11 had normal karyotypes, 1 had a chromosomal insertion in their karyotype, and 1 had the karyotype 47, XXX. To confirm the effectiveness and reliability of niPGT, eight aneuploid blastocysts from four patients were re-cultured and examined. Blastocysts were thawed using vitrified thawing solution (Kitazato Corporation, Shizuoka, Japan) under a stereomicroscope at 25◦C and individually placed in a culture dish containing 15 μl blastocyst medium for re-culture. All thawed blastocysts were cultured in an incubator (COOK, Queensland, Australia) with 6% $CO_2$, 5% $O_2$, and a humid atmosphere at 37◦C. After 14–18 h, a hole was generated in the blastocysts using a laser to release BF, and the blastocysts were moved to a biopsy dish containing 7.5 μl blastocyst medium for subsequent re-biopsy. Ten μl mixture of SCM was collected into an RNase-DNase-free PCR tube containing 5 μl cell lysis buffer (Yikon Genomics, Shanghai, China).

## Protocol for WGA

Samples of SCM, TE biopsy, and BE were placed individually into cell lysis buffer. Multiple annealing and looping-based amplification cycles was used for WGA, as described previously (Jiao *et al.*, 2019). This modified method was based on the formation of a loop structure, which prevented further amplification of full amplicons after 5–12 cycles of pre-amplification. Sequencing library preparations were combined with WGA by exponential amplification of the full amplicons. The Qubit dsDNA HS Assay kit (Life Technologies, Grand Island, NY, USA) was used to measure the DNA concentration of amplification products in a Qubit 2.0 fluorometer (Life Technologies, Grand Island, NY, USA).

## DNA sequencing

WGA products were sequenced using the Illumina Hiseq 2500 platform (Illumina, San Diego, CA, USA) with 2.0 million sequencing reads generated for each sample. High-quality reads were mapped to the human reference genome hg19. A 50% increase in read counts is an index of an increase in the chromosomal copy number from two to three, while a 50% decrease in read counts is an index of a reduction in the chromosomal copy number from two to one. Copy number variation (CNV) segments were detected by a circular binary segmentation algorithm. The R programming language was used to visualize the CNV profiles of the 23 chromosomes.

# Results

## Clinical data analysis

During the period of using aCGH, we reported a result with 20–50% aneuploid cells as 'normal embryo (possible mosaic)' (low degree) and with 50–80% aneuploid cells as 'abnormal embryo (possible mosaic)'

(high degree). A total of 47 patients with no available euploid blastocyst opted to transfer mosaic blastocysts (46 low degree and one high degree). Unexpectedly, 22 (46.8%) patients obtained clinical pregnancies and 16 (34%) achieved a healthy live birth (including the one high degree mosaic blastocyst).

With the introduction of NGS, it has replaced aCGH as the predominant method for PGT in our center. We updated the contents of the reports to display a detailed karyotype. To date, 13 patients without euploid blastocysts have undergone a low degree mosaic blastocyst transfer cycle (including five mosaic segmental blastocysts, seven mosaic whole-chromosomal blastocysts and one mosaic complex blastocyst). Of these, eight (61.5%) achieved clinical pregnancies, of which there was one case of first trimester miscarriage. This miscarriage was derived from mosaic whole-chromosomal monosomy of chromosome X (31%).

The detailed information on the two approaches is shown in Supplementary Table SI.

### Efficiency of niPGT in aneuploid embryos

As shown in Supplementary Tables SII and SIII, seven of eight BE results were actual aneuploidies. An X chromosomal duplication mosaicism in the niPGT result was found in blastocyst B#1. In addition, blastocyst D#1 exhibited a euploid result in SCM, BE, and TE re-biopsied samples. All eight chromosome copy number results of SCM showed reliable detection power.

### Efficiency of niPGT in blastocysts classified as mosaic

Given the unprecedentedly high prevalence of mosaicism and the acceptable clinical outcome of putative mosaic blastocyst transfer, we investigated whether karyotypically equivocal blastocysts actually have chromosomal mosaicism. Of the 41 blastocysts diagnosed with chromosomal mosaicism by previous TE biopsy, 21 were Day 5 and 20 were Day 6. After WGA, cell-free DNA was successfully amplified in 40 (97.6%) SCM samples, while all 41 TE re-biopsy and 41 BE samples were successfully amplified. After excluding three sequencing results with baseless multiple chromosomal abnormalities, 39 SCM, 41 BE, and 39 TE karyotype data are presented in Table I.

According to previous PGT results, 19 single segmental chromosomal mosaics, 2 double segmental chromosomal mosaics, 9 single whole chromosomal mosaics, 4 double whole chromosomal mosaics, 4 multi-whole chromosomal mosaics, and 3 complex of segmental and whole chromosomal mosaics were included. Except for one with monosomy 6 (05#2), 35 (87.5%) blastocysts actually showed euploid BE results. Another five blastocysts displayed chromosomal involvement in concordance with the corresponding previous TE biopsied results (03#1, 06#2, 08#2, 11#1, and 14#1) (Figs 1 and 2). Considering all degree mosaic results as true positives, the raw concordance rates of SCM and TE re-biopsies compared with BE were 74.4% and 82% in terms of overall ploidy and 96.2% and 97.9% per single chromosome, respectively. However, when we set a mosaicism identification threshold of 50%, as described in a recent study, to balance the sensitivity and specificity (Huang et al., 2019b), the adjusted concordance rates of SCM and TE re-biopsies compared with BE were 87.2% and 85% at the overall ploidy level and 98.8% and 98.3% at the chromosomal level, respectively (Table II).

In addition, we compared the diagnostic parameters of SCM and TE re-biopsy (Table III). At the full ploidy level, the sensitivity and false negative rates for both niPGT and re-biopsy PGT were 100% and 0, respectively. All of the six positive BE results were also positive in both SCM and TE re-biopsied results. Moreover, they showed comparable specificity and false positive rates with BE in terms of clinical ploidy status and chromosomal involvement. After adjustment of the threshold for mosaicism, the specificity of niPGT for SCM increased from 69.7% to 84.8% in terms of overall ploidy and from 96.1% to 98.9% at the chromosomal level, whereas the sensitivity of niPGT decreased from 100% to 83.3% in terms of overall ploidy and from 100% to 88.9% at the chromosomal level.

Of the 25 blastocysts containing the Y chromosome (male), blastocyst 12#1 (Fig. 3) exhibited an X chromosomal duplication mosaicism in the niPGT result. Blastocysts 3#2 (Fig. 4) and 12#2 exhibited X chromosomal duplication mosaicism in the re-biopsy PGT results. These results may be attributed to the presence of maternal contamination in either the SCM or the zona pellucida during the re-biopsy.

## Discussion

In this study, the clinical incidence of mosaicism and clinical outcomes of blastocysts classified as mosaic were analyzed retrospectively. Surprisingly, the transfer of these mosaic blastocysts resulted in a clinical pregnancy rate close to that obtained in routine PGT cycles (Munne et al., 2016). Meanwhile, studies have demonstrated the acceptable viability of mosaic blastocysts despite their apparent inferiority in comparison with euploid blastocysts. This finding raised doubts over whether these karyotypically equivocal blastocysts are actual chromosomal mosaics or are in fact false positives attributed to technical factors (Greco et al., 2015; Fragouli et al., 2017; Munne et al., 2017; Munne et al., 2020). On the other hand, with the emergence of a more attractive non-invasive technology, we deem it appropriate to understand the dynamics of mosaic blastocysts by investigating and comparing cell-free DNA and embryonic DNA.

In our data collection, we discovered a high frequency of segmental chromosomal mosaics in the context of PGT based on TE biopsy. The majority of these blastocysts were found to be euploid in BE results. Recent studies have demonstrated that segmental aneuploidies predominantly originate from mitotic errors. This was based on the low concordance rates from multifocal biopsy analysis or the investigation of frequency of segmental aneuploidy of oocytes and embryos at different developmental stages (Babariya et al., 2017; Girardi et al., 2020). This can provide a reasonable explanation for the high discrepancy between the first and second biopsies in our study. Anaphase lagging is usually concomitant with the presence of micronuclei, which encapsulate fractured chromosomes and represent a mechanism of mitotic segmental abnormality (Kort et al., 2016; Vazquez-Diez et al., 2016; Li et al., 2020). However, whether overcalling or self-correction occurs at the subsequent stage of development remains unclear. To minimize the false positive rate, Girardi and colleagues considered only uniform segmental configurations with sizes in excess of 10 Mb (Girardi et al., 2020). In spite of the view that single cell S-phase in a cell cycle containing replication domains with different copy numbers can result

**Table I Raw concordance of mosaic blastocysts in cell-free DNA for non-invasive preimplantation genetic testing versus trophectoderm re-biopsy results compared with corresponding blastocyst embryo.**

| Karyotype of parent | ID | Days | SCM (n = 39) | BE (n = 41) | TE re-biopsy (n = 39) | Previous TE biopsy |
|---|---|---|---|---|---|---|
| 46, XX, t(16; 17)(p11; p13) | 01#4 | D6 | 46, XX | 46, XX | 46, XX | −mos(X)(33%) |
| Normal karyotype | 02#1 | D6 | 46, XY | 46, XY | 46, XY | +mos(Y)(32%) |
| Normal karyotype | 05#1 | D6 | 46, XX | 46, XX | 46, XX | -mos(18)(36%)<br>-mos(22)(45%) |
| Normal karyotype | 07#2 | D5 | 46, XX | 46, XX | 46, XX | del(mos)(13)(q21.31-q34)(51.21M)(68%) |
| Normal karyotype | 07#3 | D5 | 46, XX | 46, XX | 46, XX | del(mos)(2)(p25.3-p23.3)(24.10M)(54%) |
| Normal karyotype | 07#4 | D5 | 46, XY | 46, XY | 46, XY | dup(mos)(4)(q13.3-q28.2)(57.21M)(31%) |
| 46, XX, ins(6; 18)(q25; q21q22) | 09#1 | D5 | 46, XX | 46, XX | 46, XX | -mos(10)(32%)<br>+mos(14)(33%) |
| 46, XY, t(1; 14)(p36; q24) | 10#1 | D5 | 46, XX | 46, XX | 46, XX | −mos(6)(27%) |
| 46, XY, t(1; 14)(p36; q24) | 10#2 | D5 | 46, XY | 46, XY | 46, XY | del(mos)(2)(p25.3-p24.1)(36%) |
| Normal karyotype | 13#1 | D5 | 46, XY | 46, XY | 46, XY | dup(mos)(1)(q12-q24.4)(27.45 Mb)(33%)<br>del(mos)(22)(q13.31-q13.33)(4.75 Mb)(43%) |
| 46, XY, t(15; 18)(q22; q23) | 17#1 | D6 | 46, XX | 46, XX | 46, XX | +mos(13)(62%)<br>+mos(15)(33%)<br>+mos(X)(32%) |
| 46, XX, t(1; 4)(p22; q31.3) | 18#1 | D5 | 46, XY | 46, XY | 46, XY | dup(mos)(2)(q31.3-q33.2)(35.04 Mb)(35%) |
| 45, XX, der(13; 14)(q10; q10) | 19#1 | D5 | 46, XY | 46, XY | 46, XY | dup(mos)(14)(q11.2-q31.1)(63.07 Mb)(30%) |
| 45, XX, der(13; 14)(q10; q10) | 19#2 | D6 | 46, XX | 46, XX | 46, XX | del(mos)(10)(p15.3-p11.21)(36.21 Mb)(62%) |
| 45, XX, der(13; 14)(q10; q10) | 19#3 | D5 | 46, XX | 46, XX | 46, XX | dup(mos)(5)(p15.33-p12)(45.19 Mb)(42%) |
| 45, XX, der(13; 14)(q10; q10) | 19#4 | D5 | 46, XY | 46, XY | 46, XY | +(mos)6(30%)<br>-(mos)21(32%)<br>del(mos)(5)(q11.1-q35.3)(130.29 Mb)(38%) |
| Normal karyotype | 21#1 | D6 | 46, XY | 46, XY | 46, XY | -mos(10)(33%)<br>+mos(14)(q11.2-q32.12)(73.68 Mb)(39%)<br>+mos(15)(q21.1-q26.3)(54.80 Mb)(51%) |
| 46, XY, t(11; 22)(q23; q11.2) | 22#1 | D6 | 46, XX | 46, XX | 46, XX | −mos(5)(31%) |
| Normal karyotype | 03#2 | D5 | 46, XY | 46, XY | 46, XY,+Xp(×2, mos,∼70%),<br>+Xq(×2),-Yp(×0, mos,∼70%),<br>-Yq(×0, mos,∼70%) | dup(mos)(6)(q21-q22.33)(18.31M)(37%) |
| Normal karyotype | 07#1 | D5 | 46, XX | 46, XX | 44, XX,-Xq(q22.1→q25,∼21Mb,<br>×1),-Xq(q25→q28,∼32Mb,×1),<br>-1q(q21.2→q31.2,∼40Mb,×1,<br>mos,∼40%),-10(×1),-11(×1),<br>-14q(q11.2→q32.12,∼73Mb,×1,<br>mos,∼40%) | −mos(14)(38%) |

(continued)

**Table I Continued**

| Karyotype of parent | ID | Days | SCM (n = 39) | BE (n = 41) | TE re-biopsy (n = 39) | Previous TE biopsy |
|---|---|---|---|---|---|---|
| 46, XY, t(11; 20)(q13; q13.3) | 08#1 | D5 | 46, XY | 46, XY | 46, XY,-2q(q36.3→q37.3,∼7.6 Mb, ×1),-7q(q11.21→q33,∼69Mb,×1, mos,∼50%),-7q(q33→q33, ∼5Mb,×1) | +mos(3)(29%)<br>-mos(6)(36%)<br>-mos(20)(32%)<br>-mos(22)(34%) |
| Normal karyotype | 16#1 | D5 | 46, XY | 46, XY | 46, XY,-13(×1, mos,∼40%) | −mos(17)(52%) |
| 46, XX, t(16; 17)(p11; p13) | 01#3 | D6 | 46, XX | 46, XX | N | dup(mos)(21)(q11.2-q22.13)(24.55M)(35%) |
| 46, XX, t(16; 17)(p11; p13) | 01#2 | D5 | 46, XX,-Xq(×1, mos,∼50%), +5q(×3, mos,∼50%),-6p(×1, mos,∼40%) | 46, XX | 46, XX | del(mos)(5)(q34-35.3)(19.26M)(38%) |
| 45, XX, der(13; 14)(q10; q10) | 04#1 | D6 | 46, XY,+16q(×3, mos,∼40%) | 46, XY | 46, XY | del(mos)(9)(q22.31-q34.3)(36%) |
| 47, XXX | 06#1 | D6 | 46, XY,-4q(q13.2→q35.2, ∼124Mb,×1, mos,∼40%) | 46, XY | 46, XY | dup(mos)(1)(q21.2-q44)(98.70M)(44%) |
| Normal karyotype | 12#1 | D6 | 46, XY,+Xq(×2, mos,∼40%), -2q(q14.3→q32.1,∼55Mb,×1, mos,∼30%),-2q(q32.1→q37.3, ∼59Mb,×1, mos,∼40%), +3q(q22.3→q29,∼61Mb,×3, mos,∼40%),-6q(q11.1→q22.32, ∼65Mb,×1, mos,∼30%) | 46, XY | 46, XY | del(mos)(2)(q14.3-q37.3)(114.47 Mb)(47%) |
| Normal karyotype | 15#1 | D5 | 46, XX,-3q(q11.2→q26.31, ∼81Mb,×1, mos,∼30%), +7q(q11.22→q36.3,∼91Mb,×3, mos,∼30%),-14q(q11.2→q32.12, ∼75Mb,×1, mos,∼40%) | 46, XX | 46, XX | +mos(6)(34%)<br>+mos(21)(28%)<br>-mos(22)(33%) |
| Normal karyotype | 16#2 | D5 | 46, XY,+2p(p23.1→p13.1, ∼43Mb,×3),- 13(×1, mos,∼30%) | 46, XY | 46, XY | −mos(X)(47%) |
| 45, XX, der(13; 14)(q10; q10) | 19#5 | D5 | 46, XY,+10q(q25.1→q25.3, ∼10Mb,×3) | 46, XY | 46, XY | -(mos)21(30%)<br>dup(mos)(4)(q12-q34.3)(128.01 Mb)(33%)<br>del(mos)(19)(q11-q13.11)(4.99 Mb)(47%) |
| Normal karyotype | 12#3 | D5 | N | 46, XX | 46, XX | del(mos)(1)(q31.1-q37.2)(114.47 Mb)(47%) |
| 46, XX, t(16; 17)(p11; p13) | 01#1 | D5 | 46, XY,+16p(×3, mos,∼70%) | 46, XY | 46, XY,-Yp(×0, mos,∼50%), -13q(q31.1→q32.1,∼11Mb,×1), -18q(q22.1→q22.1,∼4Mb,×1) | dup(mos)(3)(q11.1-q13.37)(20.59M)(32%)<br>dup(mos)(12)(q14.1-q22)(33.49M)(35%) |
| Normal karyotype | 12#2 | D6 | 46, XY,-7p(×1, mos,∼40%), -7q(×1, mos,∼30%),-8p(×1, mos,∼30%),+13q(q12.11→q14.3, ∼36Mb,×3, mos,∼30%), +20q(×3, mos,∼30%) | 46, XY | 46, XY,+Xp(×2, mos,∼70%),+Xq(q22.1→q28, ∼54Mb,×2, mos,∼60%),-Yp(×0, mos,∼60%),-Yq(×0, mos,∼40%) | +mos(6)(38%)<br>-mos(17)(34%) |

(continued)

**Table I Continued**

| Karyotype of parent | ID | Days | SCM (n = 39) | BE (n = 41) | TE re-biopsy (n = 39) | Previous TE biopsy |
|---|---|---|---|---|---|---|
| Normal karyotype | 20#1 | D6 | 46, XY,+3q(q11.2→q24, ∼49Mb,×3, mos,∼30%), +6q(q13→q26,∼94Mb,×3, mos,∼30%),+16p(×3, mos, ∼30%), +17p(×3, mos,∼30%), +20q(×3, mos,∼30%) | 46, XY | 46, XY,+13q(q31.1→q34,∼29Mb, ×4) | dup(mos)(6)(q21-q27)(53.86 Mb)(44%) |
| Normal karyotype | 11#2 | D6 | N/A | 46, XX | N | dup(mos)(4)(q26-q32.1)(46.51 Mb)(41%) |
| Normal karyotype | 03#1 | D6 | 45, XY,-14(×1) | 45, XY,-14(×1) | 46, XY,+9p(pter→p24.1,∼8Mb, ×3),+9p(p23→p13.2,∼26Mb,×3), +9q(q21.13→q32,∼37Mb,×3) | −mos(14)(63%) |
| 47, XXX | 06#2 | D6 | 46, XX,-7p(p22.2→p11.2,∼54Mb,×1, mos,∼40%),-16q(q12.1→q24.1,∼41Mb,×1, mos,∼30%) | 46, XX,-7q(q22.1→q36.3,∼60Mb,×1, mos,∼60%) | 46, XX,-7q(q22.1→q36.3,∼58Mb,×1) | del(mos)(7)(p22.3-q36.3)(159.11M)(66%) |
| 46, XY, t(11; 20)(q13; q13.3) | 08#2 | D6 | 46, XX,-11q(q13.4→q25,∼63Mb,×1) | 46, XX,-11q(q13.3→q25,∼64Mb,×1) | 46, XX,-11q(q13.3→q25, ∼64Mb,×1) | del(mos)(11)(q13.3-q25)(62.42M)(27%) |
| Normal karyotype | 11#1 | D6 | 46, XY,-8q(q11.1→q24.3,∼95Mb,×1, mos,∼40%),+12q(q11→q24.33, ∼94Mb,×3, mos,∼30%), -18q(q11.2→q23,∼59Mb,×1) | 45, XY,-18(×1) | 45, XY,-18(×1) | -mos(18)(59%) +mos(X)(56%) |
| 46, XX, t(11; 22)(q25; q12) | 14#1 | D6 | 46, XX,+3q(×3, mos,∼40%), +22q(q11.1→q13.32, ∼33Mb,×3, mos,∼50%) | 46, XX,+22q(q11.1→q13.32, ∼33Mb,×3, mos,∼50%) | 46, XX,+22q(q11.1→q13.32, ∼33Mb,×3, mos,∼50%) | +mos(22)(62%) |
| Normal karyotype | 05#2 | D6 | 49, XY,+3p(×3, mos,∼50%),+3q(×3),-4(×1), -6p(×1, mos,∼70%), -6q(×1, mos,∼60%),+9(×5), +11p(×3, mos,∼50%), +11q(×3, mos,∼40%),+14(×3), -16p(×1, mos,∼60%),-16q(×1, mos,∼70%),+17q(×3, mos,∼70%),+18p(×3),+18q(×3, mos,∼60%),-21(×1, mos,∼30%), -22(×1, mos,∼40%) | 43, XY,-4(×1),-6(×1), +9p(×3),+9q(q21.11→q32, ∼46Mb,×3, mos,∼70%), +9q(q32→q33.1,∼6Mb,×3), -16(×1) | 43, XY,-4(×1),-6(×1),+13q(q12.11→q30.1, ∼78Mb,×3, mos,∼30%),-16(×1) | -6(×1) -mos(4)(65%) -mos(5)(62%) -mos(16)(60%) |

niPGT, non-invasive preimplantation genetic testing; TE, trophectoderm; Days, the embryo development days of previous biopsy and vitrification; SCM, spent culture medium; BE, blastocyst embryo; N, noisy result of baseless multiple chromosomal abnormalities; N/A, no result.

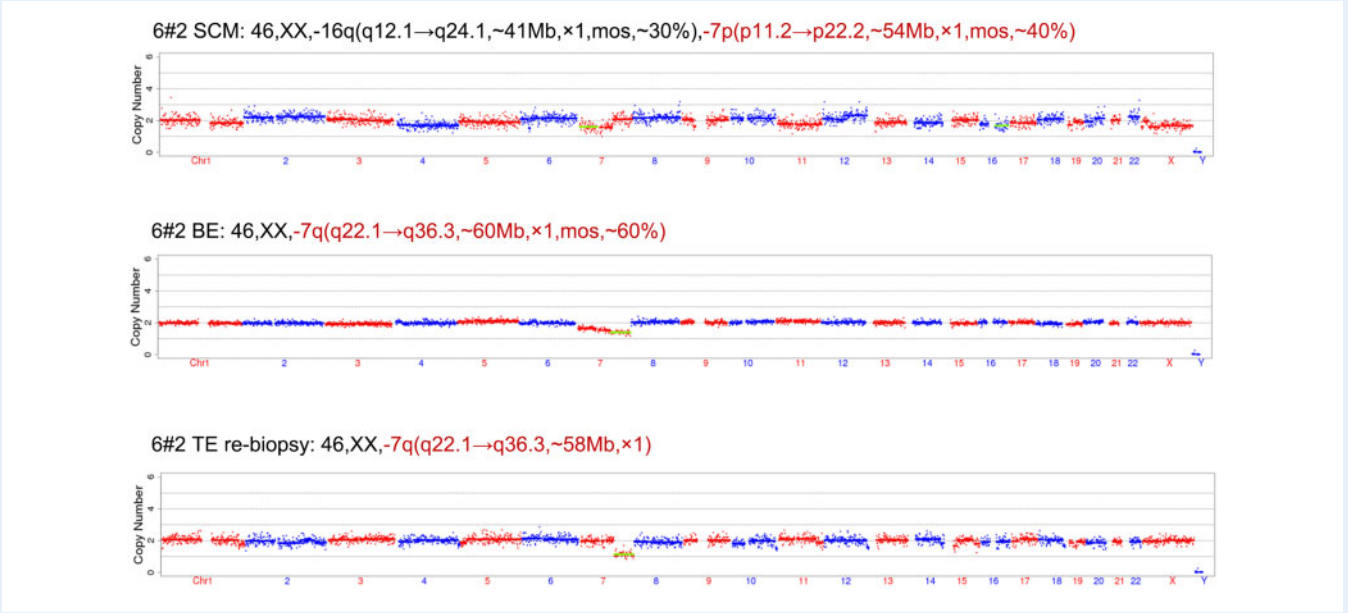


**Figure 1. Chromosome copy number profiles of an incomplete size-reciprocal segmental abnormality in SCM (-7p11.2-p22.2) and embryonic (-7q22.1-q36.3) test results compared with a previous 7p22.3-q36.3 deletion diagnosis (sample 6#2)**. SCM, spent culture medium; BE, blastocyst embryo; TE, trophectoderm.

in a segmental-like abnormality (Van der Aa *et al.*, 2013), the average size of 1.8 Mb replication domains in Epstein–Barr virus transformed lymphoblastoid cells (Ryba *et al.*, 2010) is far below the size we detected in this study. Furthermore, since G0/G1-phase cells are more prevalent than S-phase cells in cell populations (Van der Aa *et al.*, 2013), the TE biopsy in our study was conducted using a set of cells, instead of individual cells, to lower the impact of S-phase imbalances. Nevertheless, a characteristic of the rapidly dividing cells is that the G1 phase in the cell cycle is short, making it more likely for the cells to be in S-phase (Ambartsumyan and Clark, 2008).

Given the uncertainty of diagnosing mosaic segmental aneuploidy from a single TE biopsy and the potential detrimental effects of a re-biopsy on embryonic development, we conducted niPGT using cell-free DNA from blastocysts classified as having a mosaic segmental abnormality. Despite the high euploid rate of BE, which contains the ICM that will develop into the fetus proper (Taylor *et al.*, 2014), two cases (06#2 and 08#2) exhibited genuine uniform or mosaic sub-chromosomal abnormalities. Fragouli *et al.* suggested that such embryos have an implantation capacity similar to that of euploid embryos. Cells with lethal double-stranded DNA breaks may arrest or be eliminated during development, which rarely leads to severe gestational complications (Fragouli *et al.*, 2017). Nevertheless, it is a risk to transfer mosaic segmental blastocysts identified from a single biopsy, as a wide spectrum of phenotypes from completely normal to severe syndromes in patients with sub-chromosomal imbalances have been reported (Nevado *et al.*, 2014; Capalbo *et al.*, 2017a). It is worth noting that blastocyst 08#2 appeared to have uniform segmental aneuploidy of 11q13.3-q25 deletion (Fig. 2), which contains the region related to Jacobsen syndrome (Chen *et al.*, 2017). However, abnormal cells in this blastocyst only accounted for 27% of the whole blastocyst according to the previous diagnostic result. Therefore, a second round of extra-embryonic DNA examination using a minimal invasive technology is deemed an acceptable approach to maximize the use of available blastocysts and minimize the risk of an adverse pregnancy.

In our study, niPGT of putative whole chromosomal mosaic blastocysts showed reliable concordance rates with the gold standard of whole blastocyst chromosomal constitution. All blastocysts previously classified as low degree mosaics were identified as euploid via BE PGT. When the mosaicism threshold was set to 50%, all of the 11 blastocysts were euploid by niPGT except blastocyst 16#2, while three misdiagnosed re-biopsied PGT results (07#1, 08#1, and 12#2) were false positives. These cases might result from a technical artifact or biological events such as preferential allocation of abnormal cells into TE and euploid cells into ICM (Mantikou *et al.*, 2012; Capalbo and Rienzi, 2017). This result suggests that niPGT might be a more precise and attractive approach for predicting the chromosomal configurations of the embryo proper compared with TE re-biopsy. For the six high-degree mosaic blastocysts, both non-embryonic and TE re-biopsied chromosomal constitutions were well representative of reconfirmed abnormal chromosomes in the whole blastocysts. Furthermore, cell-free DNA in the SCM showed powerful detectability at the level of both a single chromosome and overall ploidy.

Recently, Bolton *et al.* built a mouse model to investigate the fate of aneuploid cells in mosaic embryos and drew the conclusion that aneuploid cells in the ICM lineage are eliminated by apoptosis and those in the TE remain viable, but proliferate with severe defects (Bolton *et al.*, 2016). According to this theory, cell-free DNA in SCM is leaked primarily from the ICM, which seems more representative of the fetal lineage. Apoptosis may not be limited to aneuploid cells. Huang *et al.* (2019a, 2019b) revealed that niPGT for aneuploid cells exhibits a higher reliability than routine PGT-A of a TE biopsy, regardless of whether the whole embryo is aneuploid or euploid. In our study,

**Table II Adjusted concordance of mosaic blastocysts in cell-free DNA for non-invasive preimplantation genetic testing versus TE re-biopsy results compared with corresponding BE.**

| Karyotype of parent | ID | Days | SCM | BE | TE re-biopsy | Previous TE biopsy |
|---|---|---|---|---|---|---|
| 46, XX, t(16; 17)(p11; p13) | 01#4 | D6 | 46, XX | 46, XX | 46, XX | −mos(X)(33%) |
| Normal karyotype | 02#1 | D6 | 46, XY | 46, XY | 46, XY | +mos(Y)(32%) |
| Normal karyotype | 05#1 | D6 | 46, XX | 46, XX | 46, XX | -mos(18)(36%) |
| | | | | | | -mos(22)(45%) |
| Normal karyotype | 07#2 | D5 | 46, XX | 46, XX | 46, XX | del(mos)(13)(q21.31-q34)(51.21M)(68%) |
| Normal karyotype | 07#3 | D5 | 46, XX | 46, XX | 46, XX | del(mos)(2)(p25.3-p23.3)(24.10M)(54%) |
| Normal karyotype | 07#4 | D5 | 46, XY | 46, XY | 46, XY | dup(mos)(4)(q13.3-q28.2)(57.21M)(31%) |
| 46, XX, ins(6; 18)(q25; q21q22) | 09#1 | D5 | 46, XX | 46, XX | 46, XX | -mos(10)(32%) |
| | | | | | | +mos(14)(33%) |
| 46, XY, t(1; 14)(p36; q24) | 10#1 | D5 | 46, XX | 46, XX | 46, XX | −mos(6)(27%) |
| 46, XY, t(1; 14)(p36; q24) | 10#2 | D5 | 46, XY | 46, XY | 46, XY | del(mos)(2)(p25.3-p24.1)(35%) |
| Normal karyotype | 13#1 | D5 | 46, XY | 46, XY | 46, XY | dup(mos)(1)(q12-q24.4)(27.45 Mb)(33%) |
| | | | | | | del(mos)(22)(q13.31-q13.33)(4.75 Mb)(43%) |
| 45, XX, der(13; 14)(q10; q10) | 04#1 | D6 | 46, XY | 46, XY | 46, XY | del(mos)(9)(q22.31-q34.3)(36%) |
| 47, XXX | 06#1 | D6 | 46, XY | 46, XY | 46, XY | dup(mos)(1)(q21.2-q44)(98.70M)(44%) |
| Normal karyotype | 12#1 | D6 | 46, XY | 46, XY | 46, XY | del(mos)(2)(q14.3-q37.3)(114.47 Mb)(47%) |
| Normal karyotype | 15#1 | D5 | 46, XX | 46, XX | 46, XX | +mos(6)(34%) |
| | | | | | | +mos(21)(28%) |
| | | | | | | -mos(22)(33%) |
| Normal karyotype | 16#1 | D5 | 46, XY | 46, XY | 46, XY | −mos(17)(52%) |
| 46, XY, t(15; 18)(q22; q23) | 17#1 | D6 | 46, XX | 46, XX | 46, XX | +mos(13)(62%) |
| | | | | | | +mos(15)(33%) |
| | | | | | | +mos(X)(32%) |
| 46, XX, t(1; 4)(p22; q31.3) | 18#1 | D5 | 46, XY | 46, XY | 46, XY | dup(mos)(2)(q31.3-q33.2)(35.04 Mb)(35%) |
| 45, XX, der(13; 14)(q10; q10) | 19#1 | D5 | 46, XY | 46, XY | 46, XY | dup(mos)(14)(q11.2-q31.1)(63.07 Mb)(30%) |
| 45, XX, der(13; 14)(q10; q10) | 19#2 | D6 | 46, XX | 46, XX | 46, XX | del(mos)(10)(p15.3-p11.21)(36.21 Mb)(62%) |
| 45, XX, der(13; 14)(q10; q10) | 19#3 | D5 | 46, XX | 46, XX | 46, XX | dup(mos)(5)(p15.33-p12)(45.19 Mb)(42%) |

(continued)

**Table II Continued**

| Karyotype of parent | ID | Days | SCM | BE | TE re-biopsy | Previous TE biopsy |
|---|---|---|---|---|---|---|
| 45, XX, der(13; 14)(q10; q10) | 19#4 | D5 | 46, XY | 46, XY | 46, XY | +(mos)6(30%)<br>-(mos)21(32%)<br>del(mos)(5)(q11.1-q35.3)(130.29 Mb)(38%) |
| Normal karyotype | 21#1 | D6 | 46, XY | 46, XY | 46, XY | -mos(10)(33%)<br>+mos(14)(q11.2-q32.12)(73.68 Mb)(39%)<br>+mos(15)(q21.1-q26.3)(54.80 Mb)(51%) |
| 46, XY, t(11; 22)(q23; q11.2) | 22#1 | D6 | 46, XX | 46, XX | 46, XX | −mos(5)(31%) |
| Normal karyotype | 03#2 | D5 | 46, XY | 46, XY | 46, XY,+Xp(×2, mos,∼70%),+Xq(×2),<br>-Yp(×0, mos,∼70%),<br>-Yq(×0, mos,∼70%) | dup(mos)(6)(q21-q22.33)(18.31M)(37%) |
| Normal karyotype | 07#1 | D5 | 46, XX | 46, XX | 44, XX,-Xq(q22.1→q25, ∼21Mb,×1),-Xq(q25→q28, ∼32Mb,×1),-10(×1),-11(×1) | −mos(14)(38%) |
| 46, XY, t(11; 20)(q13; q13.3) | 08#1 | D5 | 46, XY | 46, XY | 46, XY,-2q(q36.3→q37.3, ∼7.6 Mb,×1),<br>-7q(q11.21→q33,∼69Mb,×1, mos,∼50%),-<br>7q(q33→q33,∼5Mb,×1) | +mos(3)(29%)<br>-mos(6)(36%)<br>-mos(20)(32%)<br>-mos(22)(34%) |
| Normal karyotype | 12#2 | D6 | 46, XY | 46, XY | 46, XY,+Xp(×2, mos,∼70%), +Xq(q22.1→q28, ∼54Mb,×2, mos,∼60%), -Yp(×0, mos,∼60%) | +mos(6)(38%)<br>-mos(17)(34%) |
| Normal karyotype | 20#1 | D6 | 46, XY | 46, XY | 46, XY,+13q(q31.1→q34, ∼29Mb,×4) | dup(mos)(6)(q21-q27)(53.86 Mb)(44%) |
| 46, XX, t(16; 17)(p11; p13) | 01#3 | D6 | 46, XX | 46, XX | N | dup(mos)(21)(q11.2-q22.13)(24.55M)(35%) |
| 46, XX, t(16; 17)(p11; p13) | 01#2 | D5 | 46, XX,-Xq(×1, mos,∼50%), +5q(×3, mos,∼50%) | 46, XX | 46, XX | del(mos)(5)(q34-35.3)(19.26M)(38%) |
| Normal karyotype | 16#2 | D5 | 46, XY,+2p(p23.1→p13.1, ∼43Mb,×3) | 46, XY | 46, XY | −mos(X)(47%) |
| 45, XX, der(13; 14)(q10; q10) | 19#5 | D5 | 46, XY,+10q(q25.1→q25.3, ∼10Mb,×3) | 46, XY | 46, XY | -(mos)21(30%)<br>dup(mos)(4)(q12-q34.3)(128.01 Mb)(33%)<br>del(mos)(19)(q11-q13.11)(4.99 Mb)(47%) |

(continued)

**Table II Continued**

| Karyotype of parent | ID | Days | SCM | BE | TE re-biopsy | Previous TE biopsy |
|---|---|---|---|---|---|---|
| Normal karyotype | 12#3 | D5 | N | 46, XX | 46, XX | del(mos)(1)(q31.1-q37.2)(114.47 Mb)(47%) |
| 46, XX, t(16; 17)(p11; p13) | 01#1 | D5 | 46, XY,+16p(×3, mos,∼70%) | 46, XY | 46, XY,-Yp(×0, mos,∼50%), -13q(q31.1→q32.1,∼11Mb,×1), -18q(q22.1→q22.1,∼4Mb,×1) | dup(mos)(3)(q11.1-q13.37)(20.59M)(32%)<br>dup(mos)(12)(q14.1-q22)(33.49M)(35%) |
| Normal karyotype | 11#2 | D6 | N/A | 46, XX | N | dup(mos)(4)(q26-q32.1)(46.51 Mb)(41%) |
| Normal karyotype | 03#1 | D6 | 45, XY,-14(×1) | 45, XY,-14(×1) | 46, XY,+9p(pter→p24.1,∼8Mb,×3), +9p(p23→p13.2,∼26Mb,×3), +9q(q21.13→q32,∼37Mb,×3) | −mos(14)(63%) |
| 46, XY, t(11; 20)(q13; q13.3) | 08#2 | D6 | 46, XX,-11q(q13.4→q25, ∼63Mb,×1) | 46, XX,-11q(q13.3→q25,∼64Mb,×1) | 46, XX,-11q(q13.3→q25,∼64Mb,×1) | del(mos)(11)(q13.3-q25)(62.42M)(27%) |
| Normal karyotype | 11#1 | D6 | 46, XY,-18q(q11.2→q23, ∼59Mb,×1) | 45, XY,-18(×1) | 45, XY,-18(×1) | -mos(18)(59%)<br>+mos(X)(56%) |
| 46, XX, t(11; 22)(q25; q12) | 14#1 | D6 | 46, XX,+22q(q11.1→q13.32, ∼33Mb,×3, mos,∼50%) | 46, XX,+22q(q11.1→q13.32,∼33Mb, ×3, mos,∼50%) | 46, XX,+22q(q11.1→q13.32, ∼33Mb,×3, mos,∼50%) | +mos(22)(62%) |
| Normal karyotype | 05#2 | D6 | 49, XY,+3p(×3, mos,∼50%),+3q(×3),-4(×1), -6p(×1, mos,∼70%),-6q(×1, mos,∼60%),+9(×5),+11p(×3, mos,∼50%),+14(×3),-16p(×1, mos,∼60%),-16q(×1, mos,∼70%),+17q(×3, mos,∼70%),+18p(×3),+18q(×3, mos,∼60%) | 43, XY,-4(×1),-6(×1),+9p(×3), +9q(q21.11→q32,∼46Mb,×3, mos, ∼70%),+9q(q32→q33.1,∼6Mb,×3),-16(×1) | 43, XY,-4(×1),-6(×1),-16(×1) | -6(×1)<br>-mos(4)(65%)<br>-mos(5)(62%)<br>-mos(16)(60%) |
| 47, XXX | 06#2 | D6 | 46, XX | 46, XX,-7q(q22.1→q36.3,∼60Mb, ×1, mos,∼60%) | 46, XX,-7q(q22.1→q36.3, ∼58Mb,×1) | del(mos)(7)(p22.3-q36.3)(159.11M)(66%) |

A mosaicism threshold of 50% was set to balance the sensitivity and specificity.

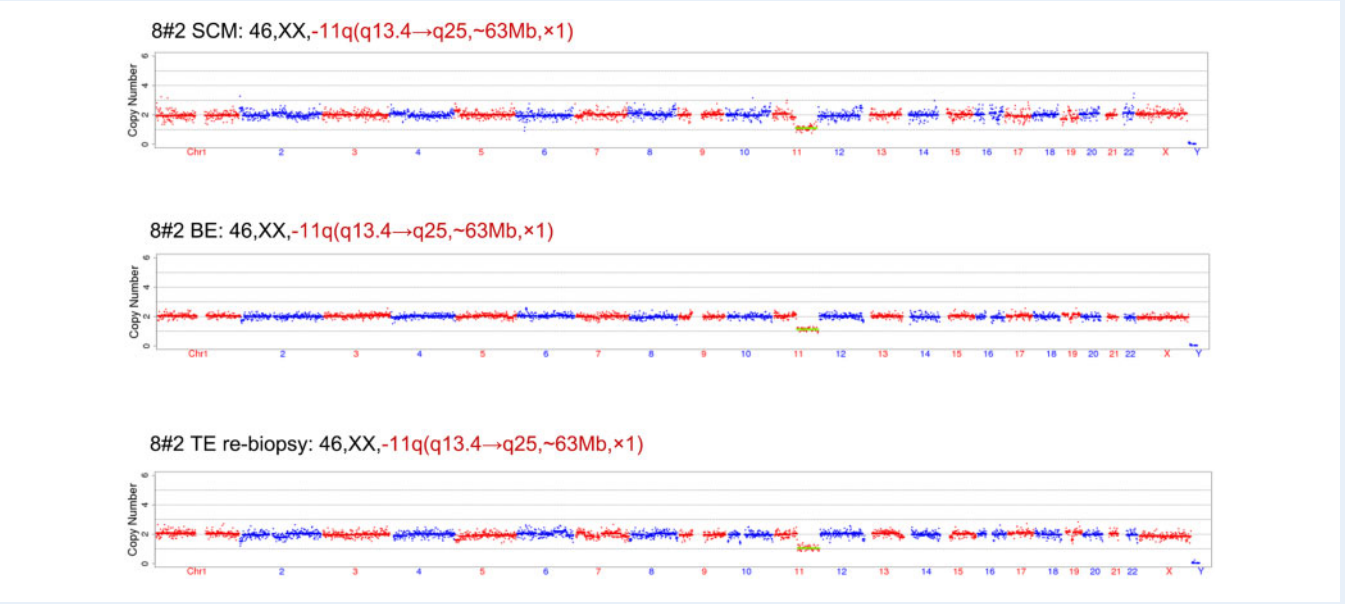


**Figure 2. Chromosome copy number profiles of uniform segmental aneuploidy of 11q13.3-q25 deletion in BE, TE re-biopsy and corresponding SCM (sample 8#2)**. SCM, spent culture medium; BE, blastocyst embryo; TE, trophectoderm.

**Table III Comparison of the diagnostic parameters of SCM and TE re-biopsy.**

| | | | Concordance | Sensitivity | Specificity | FPR | FNR | PPV | NPV | PLR | NLR | DOR |
|---|---|---|---|---|---|---|---|---|---|---|---|---|
| Raw | SCM (n = 27) | Per overall ploidy | 74.4% | 100% | 69.7% | 30.3% | 0 | 37.5% | 100% | 3.3 | 0 | – |
| | | Per single chromosome | 96.2% | 100% | 96.1% | 3.9% | 0 | 20% | 100% | 25.8 | 0 | – |
| | Re-biopsy (n = 27) | Per overall ploidy | 82% | 100% | 78.8% | 21.2% | 0 | 46.2% | 100% | 4.7 | 0 | – |
| | | Per single chromosome | 98.0% | 77.8% | 98.1% | 1.9% | 22.2% | 28% | 99.8% | 40.1 | 0.2 | 176.8 |
| Adjusted | SCM (n = 27) | Per overall ploidy | 87.2% | 83.3% | 84.9% | 15.2% | 16.7% | 50% | 96.6% | 5.5 | 0.2 | 28 |
| | | Per single chromosome | 98.8% | 88.9% | 98.9% | 1.1% | 11.1% | 44.4% | 99.6% | 82.4 | 0.1 | 733.6 |
| | re-biopsy (n = 27) | Per overall ploidy | 85% | 100% | 81.8% | 18.2% | 0 | 50% | 100% | 5.5 | 0 | – |
| | | Per single chromosome | 98.3% | 77.8% | 98.5% | 1.5% | 22.2% | 33.3% | 99.8% | 51.5 | 0.2 | 228.3 |

Sensitivity, (true positives)/(true positives + false negatives); Specificity, (true negatives)/(true negatives + false positives); FPR, false positive rate = (false positives)/(true negatives + false positives); FNR, false negative rate = (false negatives)/(true positives + false negatives); PPV, positive predictive value = (true positives)/(true positives + false positives); NPV, negative predictive value = (true negatives)/(true negatives + false negatives); PLR, positive likelihood ratio = Sensitivity/FPR; NLR, negative likelihood ratio = FNR/Specificity; DOR, diagnostic odds ratio = (true positives * true negatives)/(false positives * false negatives).

blastocyst 12#1 displayed a euploid embryonic chromosome complement in both BE and TE re-biopsy, while a mosaic segmental aneuploidy of 2q14.3-q37.3 was detected in the non-embryonic culture medium (Fig. 3), which had been tested in the original TE biopsy cycle. Nevertheless, this mosaic segment disappeared when we considered a mosaicism threshold of 50%. A similar result was obtained for embryo 06#2 (Fig. 1), which showed an incomplete size-reciprocal segmental abnormality in extra-embryonic (-7p11.2-p22.2) and embryonic (-7q22.1-q36.3) testing results compared with previous diagnosis results (-7p22.3-q36.3). When the mosaicism threshold was used, the niPGT result appeared as a false negative. This observation suggested that some DNA fragments may leak from the embryo to non-embryonic medium during re-culture development. The failure to detect corresponding abnormalities in the culture media can be explained as follows. First, the previously detected aneuploid cells indeed existed and subsequently underwent apoptosis and degradation, during which leaked DNA was released into BF and SCM. However, the apoptotic euploid cells far outnumbered aneuploid cells owing to their dominant proportion and the DNA released from aneuploid cells degraded below the detectable threshold when we collected the culture media. Second, amplification noise led to the high mosaic rate in previous results and the second testing countered these false positive errors. Regardless, niPGT after 14–18 h re-culture was found to be a superior option for the best use of blastocysts.

This study is the first to explore the practicability of niPGT in the diagnostic reassessment of putative mosaicism. To our knowledge, mosaicism is believed to be a grey area in the context of PGT-A (Capalbo *et al.*, 2017b; Vera-Rodriguez and Rubio, 2017). Reports of a

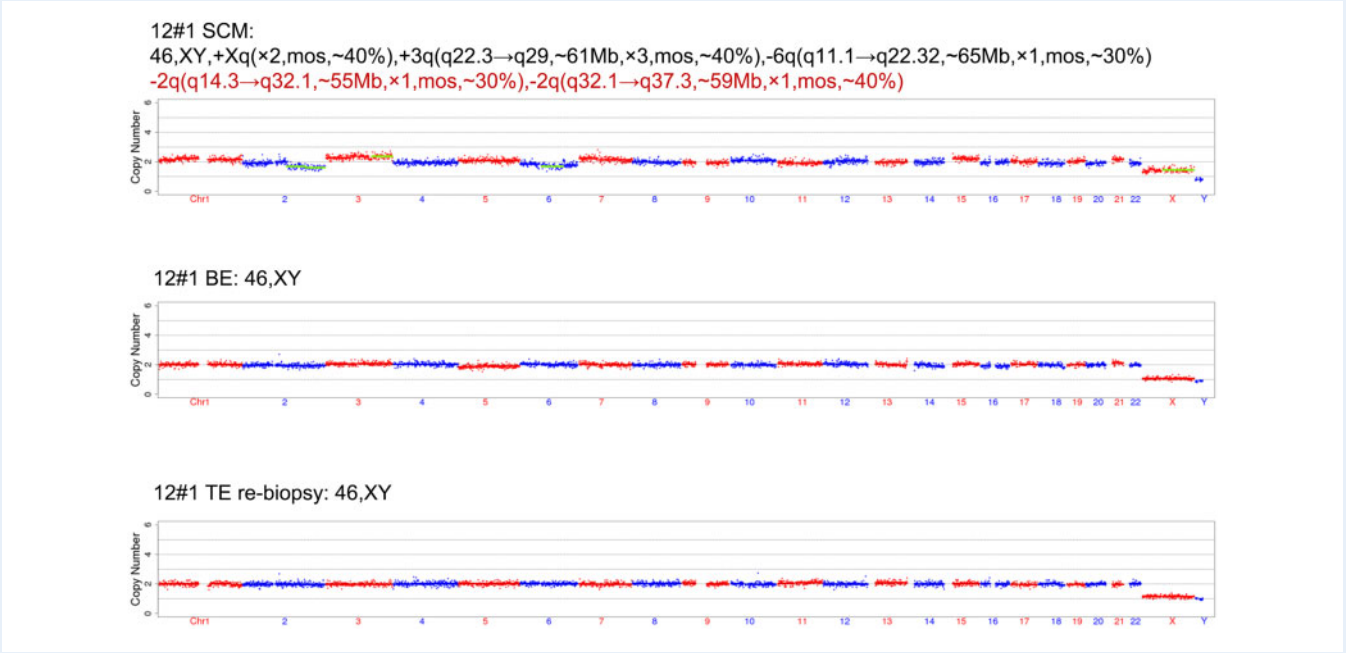


**Figure 3. Chromosome copy number profiles of euploid BE, TE re-biopsy and mosaic segmental aneuploid SCM which were detected in a previous biopsy result [del(mos)(2)(q14.3-q37.3)(114.47)(47%)] (sample 12#1)**. SCM, spent culture medium; BE, blastocyst embryo; TE, trophectoderm.

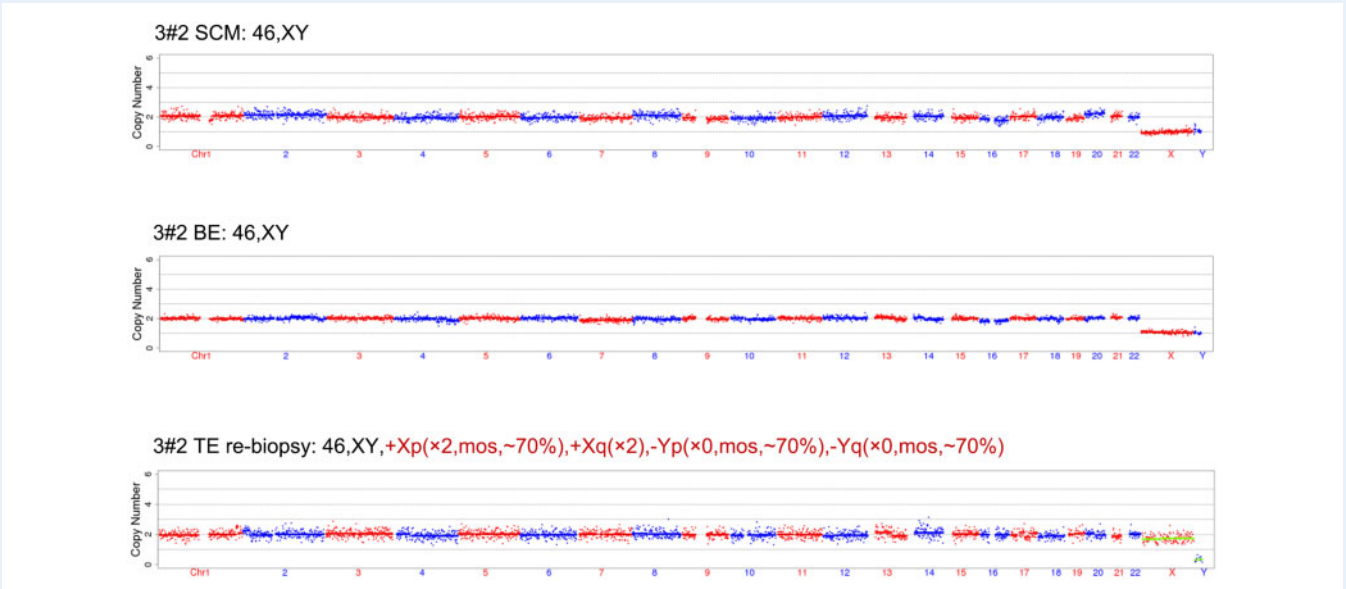


**Figure 4. Chromosome copy number profiles of euploid male BE and SCM, and TE re-biopsy of a sex chromosomal aneuploid resulting from possible maternal contamination (sample 3#2)**. SCM, spent culture medium; BE, blastocyst embryo; TE, trophectoderm.

high incidence of mosaic blastocysts in PGT-A cycles reduce the number of blastocysts available for transfer, thereby affecting overall clinical outcomes. This is particularly concerning for those patients who have no euploid blastocysts. The present study suggests a novel opportunity for these patients: regardless of the technical or biological basis of mosaicism, niPGT is a viable option for testing re-cultured blastocysts. Furthermore, the karyotypes of couples also need to be considered. The diagnostic viability of niPGT makes it applicable not only to putative mosaic blastocysts, but also to those embryos with no amplified DNA result, considering the unacceptable amplification failure rate in

our study (2%) and of others (2.5%) (Cimadomo *et al.*, 2018). The primary limitation of this study is the small sample size, which decreases the strength of our conclusions. If possible, determining the clinical outcome of niPGT of reassessed mosaic blastocysts would provide further information in this field. Larger scale and well-designed studies testing embryo-derived and extra-embryonic genetic material are warranted to shed light on the mechanism and potential dynamics of mosaic embryos.

## Supplementary data

Supplementary data are available at *Human Reproduction* online.

## Data availability

The data underlying this article will be shared on reasonable request to the corresponding author.

## Acknowledgements

The authors wish to acknowledge Sijia Lu and Jieliang Ma (Yikon Genomics) for their assistance with the data analysis. The authors are grateful to patients who donated their embryos for our study.

## Authors' roles

P.Z. and Z.G.Z. designed the experiments. X.Y.L. and Y.H. performed the experiment and wrote the manuscript. D. W. C. and W.B.Z. analyzed the statistical data. D.M.J. assisted embryo biopsy and vitrified thawing. X.Q.Z. collated patients data. Z.L.W. reviewed the data statistic. Y.X.C. revised the manuscript.

## Funding

This work was supported by grants from National Key Technology Research and Development Program of China (No. 2017YFC1002004), the Central Guiding the Science and Technology Development of the Local (2018080802D0081), and College Natural Science Project of Anhui Province (KJ2019A0287).

## Conflict of interest

No competing interests declared.

## References

Ambartsumyan G, Clark AT. Aneuploidy and early human embryo development. *Hum Mol Genet* 2008;**17**:R10–R15.

Babariya D, Fragouli E, Alfarawati S, Spath K, Wells D. The incidence and origin of segmental aneuploidy in human oocytes and preimplantation embryos. *Hum Reprod* 2017;**32**:2549–2560.

Bolton H, Graham S, Van der Aa N, Kumar P, Theunis K, Fernandez GE, Voet T, Zernicka-Goetz M. Mouse model of chromosome mosaicism reveals lineage-specific depletion of aneuploid cells and normal developmental potential. *Nat Commun* 2016;**7**:11165.

Capalbo A, Rienzi L. Mosaicism between trophectoderm and inner cell mass. *Fertil Steril* 2017;**107**:1098–1106.

Capalbo A, Rienzi L, Ubaldi FM. Diagnosis and clinical management of duplications and deletions. *Fertil Steril* 2017a;**107**:12–18.

Capalbo A, Romanelli V, Patassini C, Poli M, Girardi L, Giancani A, Stoppa M, Cimadomo D, Ubaldi FM, Rienzi L. Diagnostic efficacy of blastocoel fluid and spent media as sources of DNA for preimplantation genetic testing in standard clinical conditions. *Fertil Steril* 2018;**110**:870–879.

Capalbo A, Ubaldi FM, Rienzi L, Scott R, Treff N. Detecting mosaicism in trophectoderm biopsies: current challenges and future possibilities. *Hum Reprod* 2017b;**32**:492–498.

Chen CP, Wang LK, Wu PC, Chang TY, Chern SR, Wu PS, Chen YN, Chen SW, Lee CC, Yang CW. *et al.* Molecular cytogenetic characterization of Jacobsen syndrome (11q23.3-q25 deletion) in a fetus associated with double outlet right ventricle, hypoplastic left heart syndrome and ductus venosus agenesis on prenatal ultrasound. *Taiwan J Obstet Gynecol* 2017;**56**:102–105.

Chuang TH, Hsieh JY, Lee MJ, Lai HH, Hsieh CL, Wang HL, Chang YJ, Chen SU. Concordance between different trophectoderm biopsy sites and the inner cell mass of chromosomal composition measured with a next-generation sequencing platform. *Mol Hum Reprod* 2018;**24**:593–601.

Cimadomo D, Rienzi L, Romanelli V, Alviggi E, Levi-Setti PE, Albani E, Dusi L, Papini L, Livi C, Benini F. *et al.* Inconclusive chromosomal assessment after blastocyst biopsy: prevalence, causative factors and outcomes after re-biopsy and re-vitrification. A multicenter experience. *Hum Reprod* 2018;**33**:1839–1846.

De Rycke M, Goossens V, Kokkali G, Meijer-Hoogeveen M, Coonen E, Moutou C. ESHRE PGD Consortium data collection XIV-XV: cycles from January 2011 to December 2012 with pregnancy follow-up to October 2013. *Hum Reprod* 2017;**32**:1974–1994.

Elshewy N, Ji D, Zhang Z, Chen D, Chen B, Xue R, Wu H, Wang J, Zhou P, Cao Y. Association between mild stimulated IVF/M cycle and early embryo arrest in sub fertile women with/without PCOS. *Reprod Biol Endocrinol* 2020;**18**:71.

Fragouli E, Alfarawati S, Spath K, Babariya D, Tarozzi N, Borini A, Wells D. Analysis of implantation and ongoing pregnancy rates following the transfer of mosaic diploid-aneuploid blastocysts. *Hum Genet* 2017;**136**:805–819.

Gardner DK, Vella P, Lane M, Wagley L, Schlenker T, Schoolcraft WB. Culture and transfer of human blastocysts increases implantation rates and reduces the need for multiple embryo transfers. *Fertil Steril* 1998;**69**:84–88.

Girardi L, Serdarogullari M, Patassini C, Poli M, Fabiani M, Caroselli S, Coban O, Findikli N, Boynukalin FK, Bahceci M. *et al.* Incidence, origin, and predictive model for the detection and clinical management of segmental aneuploidies in human embryos. *Am J Hum Genet* 2020;**106**:525–534.

Gleicher N, Metzger J, Croft G, Kushnir VA, Albertini DF, Barad DH. A single trophectoderm biopsy at blastocyst stage is mathematically unable to determine embryo ploidy accurately enough for clinical use. *Reprod Biol Endocrinol* 2017;**15**:33.

Greco E, Minasi MG, Fiorentino F. Healthy babies after intrauterine transfer of mosaic aneuploid blastocysts. *N Engl J Med* 2015;**373**: 2089–2090.

Huang L, Lu S, Racowsky C, Xie XS. Reply to Gleicher and Barad: noninvasive preimplantation genetic testing may provide the solution to the problem of embryo mosaicism. *Proc Natl Acad Sci U S A* 2019a;**116**:21978–21979.

Huang L, Bogale B, Tang Y, Lu S, Xie XS, Racowsky C. Noninvasive preimplantation genetic testing for aneuploidy in spent medium may be more reliable than trophectoderm biopsy. *Proc Natl Acad Sci U S A* 2019b;**116**:14105–14112.

Jiao J, Shi B, Sagnelli M, Yang D, Yao Y, Li W, Shao L, Lu S, Li D, Wang X. Minimally invasive preimplantation genetic testing using blastocyst culture medium. *Hum Reprod* 2019;**34**:1369–1379.

Kort DH, Chia G, Treff NR, Tanaka AJ, Xing T, Vensand LB, Micucci S, Prosser R, Lobo RA, Sauer MV. *et al*. Human embryos commonly form abnormal nuclei during development: a mechanism of DNA damage, embryonic aneuploidy, and developmental arrest. *Hum Reprod* 2016;**31**:312–323.

Leaver M, Wells D. Non-invasive preimplantation genetic testing (niPGT): the next revolution in reproductive genetics? *Hum Reprod Update* 2020;**26**:16–42.

Li X, Hao Y, Elshewy N, Zhu X, Zhang Z, Zhou P. The mechanisms and clinical application of mosaicism in preimplantation embryos. *J Assist Reprod Genet* 2020;**37**:497–508.

Liu J, Wang W, Sun X, Liu L, Jin H, Li M, Witz C, Williams D, Griffith J, Skorupski J. *et al*. DNA microarray reveals that high proportions of human blastocysts from women of advanced maternal age are aneuploid and mosaic. *Biol Reprod* 2012;**87**:148.

Magli MC, Pomante A, Cafueri G, Valerio M, Crippa A, Ferraretti AP, Gianaroli L. Preimplantation genetic testing: polar bodies, blastomeres, trophectoderm cells, or blastocoelic fluid? *Fertil Steril* 2016;**105**:676–683.

Mantikou E, Wong KM, Repping S, Mastenbroek S. Molecular origin of mitotic aneuploidies in preimplantation embryos. *Biochim Biophys Acta* 2012;**1822**:1921–1930.

Munne S, Blazek J, Large M, Martinez-Ortiz PA, Nisson H, Liu E, Tarozzi N, Borini A, Becker A, Zhang J. *et al*. Detailed investigation into the cytogenetic constitution and pregnancy outcome of replacing mosaic blastocysts detected with the use of high-resolution next-generation sequencing. *Fertil Steril* 2017;**108**:62–71.

Munne S, Grifo J, Wells D. Mosaicism: "survival of the fittest" versus "no embryo left behind". *Fertil Steril* 2016;**105**:1146–1149.

Munne S, Spinella F, Grifo J, Zhang J, Beltran MP, Fragouli E, Fiorentino F. Clinical outcomes after the transfer of blastocysts characterized as mosaic by high resolution Next Generation Sequencing- further insights. *Eur J Med Genet* 2020;**63**:103741.

Nevado J, Mergener R, Palomares-Bralo M, Souza KR, Vallespin E, Mena R, Martinez-Glez V, Mori MA, Santos F, Garcia-Minaur S. *et al*. New microdeletion and microduplication syndromes: a comprehensive review. *Genet Mol Biol* 2014;**37**:210–219.

Palini S, Galluzzi L, De Stefani S, Bianchi M, Wells D, Magnani M, Bulletti C. Genomic DNA in human blastocoele fluid. *Reprod Biomed Online* 2013;**26**:603–610.

Popovic M, Dhaenens L, Boel A, Menten B, Heindryckx B. Chromosomal mosaicism in human blastocysts: the ultimate diagnostic dilemma. *Hum Reprod Update* 2020;**26**:313–334.

Rubio C, Navarro-Sánchez L, García-Pascual CM, Ocali O, Cimadomo D, Venier W, Barroso G, Kopcow L, Bahçeci M, Kulmann MIR. *et al*. Multicenter prospective study of concordance between embryonic cell-free DNA and trophectoderm biopsies from 1301 human blastocysts. *Am J Obstet Gynecol* 2020;**223**:751.e1–751.e13.

Ryba T, Hiratani I, Lu J, Itoh M, Kulik M, Zhang J, Schulz TC, Robins AJ, Dalton S, Gilbert DM. Evolutionarily conserved replication timing profiles predict long-range chromatin interactions and distinguish closely related cell types. *Genome Res* 2010;**20**:761–770.

Taylor TH, Gitlin SA, Patrick JL, Crain JL, Wilson JM, Griffin DK. The origin, mechanisms, incidence and clinical consequences of chromosomal mosaicism in humans. *Hum Reprod Update* 2014;**20**: 571–581.

Van der Aa N, Cheng J, Mateiu L, Zamani EM, Kumar P, Dimitriadou E, Vanneste E, Moreau Y, Vermeesch JR, Voet T. Genome-wide copy number profiling of single cells in S-phase reveals DNA-replication domains. *Nucleic Acids Res* 2013;**41**:e66.

Vazquez-Diez C, Yamagata K, Trivedi S, Haverfield J, FitzHarris G. Micronucleus formation causes perpetual unilateral chromosome inheritance in mouse embryos. *Proc Natl Acad Sci U S A* 2016;**113**: 626–631.

Vera-Rodriguez M, Michel CE, Mercader A, Bladon AJ, Rodrigo L, Kokocinski F, Mateu E, Al-Asmar N, Blesa D, Simon C. *et al*. Distribution patterns of segmental aneuploidies in human blastocysts identified by next-generation sequencing. *Fertil Steril* 2016; **105**:1047–1055.

Vera-Rodriguez M, Rubio C. Assessing the true incidence of mosaicism in preimplantation embryos. *Fertil Steril* 2017;**107**:1107–1112.

Xu J, Fang R, Chen L, Chen D, Xiao JP, Yang W, Wang H, Song X, Ma T, Bo S. *et al*. Noninvasive chromosome screening of human embryos by genome sequencing of embryo culture medium for in vitro fertilization. *Proc Natl Acad Sci U S A* 2016;**113**:11907–11912.

Yeung Q, Zhang YX, Chung J, Lui WT, Kwok Y, Gui B, Kong G, Cao Y, Li TC, Choy KW. A prospective study of non-invasive preimplantation genetic testing for aneuploidies (NiPGT-A) using next-generation sequencing (NGS) on spent culture media (SCM). *J Assist Reprod Genet* 2019;**36**:1609–1621.